Molecular Crystals and Liquid Crystals

Publication details, including instructions for authors and subscription information:
http://www.tandfonline.com/loi/gmcl20

Exciton and Polaron Contributions to Photocurrent in MeLPPP on a Picosecond Time Scale

A. Devižis [a] , A. Serbenta [a] , D. Hertel [b] & V. Gulbinas [a]

[a] Institute of Physics. Savanoriu, Vilnius, Lithuania

[b] Department of Chemistry, Physical Chemistry, University of Cologne, Cologne, Germany

Version of record first published: 06 Jul 2012

To cite this article: A. Devižis, A. Serbenta, D. Hertel & V. Gulbinas (2008): Exciton and Polaron Contributions to Photocurrent in MeLPPP on a Picosecond Time Scale, Molecular Crystals and Liquid Crystals, 496:1, 16-24

To link to this article: http://dx.doi.org/10.1080/15421400802451345

Mol. Cryst. Liq. Cryst., Vol. 496, pp. 16–24, 2008

ISSN: 1542-1406 print/1563-5287 online
DOI: 10.1080/15421400802451345

Taylor & Francis
Taylor & Francis Group

Exciton and Polaron Contributions to Photocurrent in MeLPPP on a Picosecond Time Scale

A. Devižis[1], A. Serbenta[1], D. Hertel[2], and V. Gulbinas[1]
[1]Institute of Physics. Savanoriu, Vilnius, Lithuania
[2]Department of Chemistry, Physical Chemistry, University of Cologne, Cologne, Germany

Electric field-induced second harmonic generation was applied to probe the electric field dynamics in methyl-substituted ladder-type poly(para-phenylene) (MeLPPP). To delineate the exciton and polaron contributions to the ultrafast field dynamics, we have investigated devices with traps and without them. The traps were induced upon deliberate oxidation. The relative exciton contribution to the field dynamics is larger in oxidized films due to a lower yield of mobile charge carriers.

Keywords: charge carrier; conjugated polymer; electric field; exciton

INTRODUCTION

Development of optoelectrical devices based on organic materials requires knowledge of their optical and electrical characteristics. A crucial property for the improvement of materials is the charge carrier mobility. In amorphous organic materials, the carrier mobility is much lower than that in inorganic semiconductors, typically being of the order of 1–10 cm^2/Vs in molecular crystals and 10^{-6}–10^{-3} cm^2/Vs [1] in molecular glasses and polymers. It depends on the electric field, temperature [2,3,4], and carrier density [5]. Due to the disordered nature of organic materials, it also changes with time having passed after a charge carrier was generated or injected. This dynamics becomes particularly important with minimization of devices, when their dimensions are on the nanometer length scale or

This work was supported by the Lithuanian Science and Studies Foundation. D. H. would like to thank Prof. K. Meerholz for his support and the DFG for funding.

Address correspondence to V. Gulbinas, Institute of Physics, Savanoriu ave. 231, Vilnius 02300, Lithuania. E-mail: vidgulb@ktl.mii.lt

even approach the molecular dimensions for more advanced future single-molecule-based devices. Electrical events at such small distances become very fast determined by intramolecular and intermolecular charge transfer and molecular polarization. On the ultrashort time scale, when charge carriers move at molecular distances, their drift can be comparable to the charge separation due to the polarization of the ground state and excited molecules. This displacement current related to the dielectric constant modified upon photoexcitation of the material can be comparable or even larger than the conduction current. The conduction current is caused by mobile charge carriers (polarons). In order to gain insight to transport processes on ultrafast time scales, one has to differentiate between both contributions. Several methods have been developed to measure the carrier mobility and the drift dynamics on an ultrafast time scale, such as pulse-radiolysis induced time-resolved microwave conductivity (TRMC) [6], terahertz spectroscopy [7], and the electric field probing by means of the Stark-shifted transient absorption [8]. In our investigation of the initial charge carrier separation in MeLPPP, we have clearly observed and separated the exciton and polaron contributions to the overall conductivity [9]. However, on the contrary, Heeger et al. drew conclusion that the displacement (exciton) current in PPV is negligible [10]. In a more recent study of the initial carrier mobility in 6,6-Phenyl C_{61}-butyric acid methyl ester (PCBM) by Cabanillas-Gonzalez et al. [11], the displacement current contribution was ignored. Surprisingly, they found a constant mobility on the ps time scale neglecting the extraction of carriers from the sample. Recently, we have introduced the electric field-induced time-resolved second harmonic generation (TREFISH) to probe the charge transport with ultrashort optical pulses [12]. This method is more universal than the Stark-shift method, and the experimental data are directly related to the electric field kinetics. Here, we report the investigation of exciton and polaron contributions to the conductivity in devices of MeLPPP. We used the formation of traps upon deliberate oxidation to differentiate between both components.

EXPERIMENTAL DETAILS

MeLPPP was synthesized as described in [13]. The polymer films were deposited on the indium-tin oxide (ITO) covered glass by spin coating from a toluene solution, followed by the deposition of an aluminum top electrode. The polymer film thickness was 100 nm. Some of the films have been capsulated by covering them with a thin glass plate in nitrogen atmosphere. The samples were kept in dark before experiments.

The electric field dynamics was investigated by means of the second harmonic generation method described in more details elsewhere [12]. Briefly, a Ti-saphire laser generating pulses of about 120 fs in duration at the 1-kHz repetition rate was used. The polymer films were excited by 460-nm pulses produced by the second harmonic generation of the main laser radiation with a shift of the frequency by means of Raman scattering in ethanol (460 nm). The main laser radiation pulses at 810 nm delayed with variable delay time relative to excitation pulses were used for the sample probing. The second harmonic of the probe pulse was generated in the polymer film when the electric field was applied. The second harmonic intensity is proportional to the second power of the electric field giving a possibility to investigate the electric field kinetics inside the polymer film by measuring the second harmonic intensity. The samples form a plate capacitor which is charged by about 10-μs electrical pulses applied before each optical pulse. A positive bias was applied to aluminum to avoid the charge carrier injection. The capacitor was partly discharged by the photocurrent created by the excitation pulse. Because of the 150-Ω resistor in the sample charging circuit, the sample recharging time was much longer than the time interval of our investigation. Thus, the electric field dynamics inside the polymer material was directly related to the excitation pulse created photocurrent.

The transient absorption at 810 nm was investigated simultaneously by measuring the intensity of a reflected main laser radiation probe pulse.

RESULTS AND DISCUSSION

Electric Field Dynamics

The second harmonic (I_{2H}) generation efficiency in a MeLPPP film without the applied field is close to zero. The nonzero generation efficiency in unbiased devices is caused by the contact potential difference of the device electrodes created by the work functions of Al and ITO, which equals to about 0.6 V. The I_{2H} intensity with the applied field was proportional to the square of the sum of the applied voltage and the contact potential. Upon photoexcitation, the I_{2H} intensity of the sample decreases due to the photocurrent, which partly discharges the sample capacitor. Figure 1a shows the I_{2H} intensity normalized to that without sample excitation as a function of the delay time between 460-nm excitation and 810-nm probe pulses. The I_{2H} intensity kinetics strongly depends on the applied voltage. At a low applied voltage (3 V), the I_{2H} intensity decrease is limited by the excitation pulse duration,

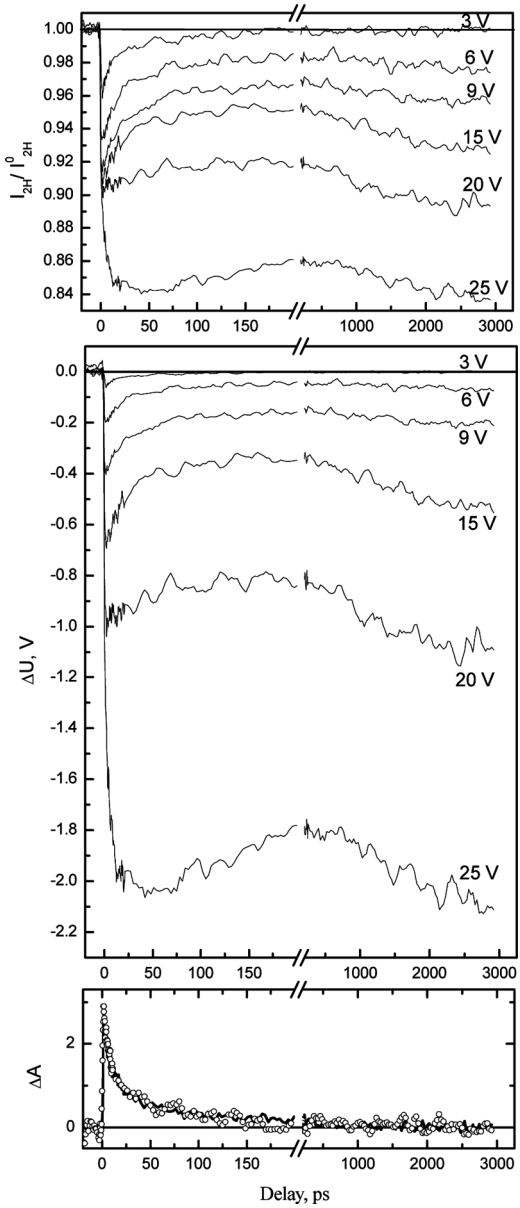

FIGURE 1 (a) I_{2H} intensity kinetics in a capsulated MeLPPP sample measured at different applied voltages; (b) calculated kinetics of the internal field; (c) electric field kinetics measured at 3 V of the applied voltage (solid line) and the transient absorption kinetics at 810 nm. The electric field kinetics was normalized to the transient absorption kinetics.

and it recovers on a ps time scale. By increasing the applied voltage, the $I_{2\mathrm{H}}$ intensity drops down again on a ns time scale. Figure 1b shows the electric field kinetics inside the polymer film calculated from the normalized second harmonic intensity kinetics as

$$\Delta E \approx \left| (I_{2H}/I_{2H}^0)^{1/2} - 1 \right| E_0. \tag{1}$$

Here, E_0 is the applied voltage, and $I^0{}_{2H}$ is the second harmonic intensity without excitation. The electric field, respectively as the I_{2H} intensity, is reduced during the optical pulse before it recovers. At higher applied voltages, the electric field decreases again on a ns time scale. The electric field kinetics and its complex dependence on the applied voltage are caused by contributions from the polaron conductivity and polarization (exciton) displacement currents related to several transient states created by photoexcitation in an electric field. The major excitations are: a) excitons, b) charge pair states created by field-assisted exciton splitting, c) charge pair states created by field-free exciton splitting on impurities and/or defects, and d) mobile electron and hole polarons. Mobile electron and hole polarons create the photocurrent, while the other states change the dielectric susceptibility of the material and contribute to the displacement current. Both the photoconductivity and displacement currents change the electric field inside the sample. The electric field dynamics can be described as

$$\begin{aligned} \Delta E(t) \approx & -[n_e(t)\Delta\alpha_{ex} + n_{cpi}(t)\Delta\alpha_{cpi})]E_{ap}/2\varepsilon\varepsilon_0 \\ & -[n_{cpf}(t)ql_p - n_p(t)ql(t)]/\varepsilon\varepsilon_0. \end{aligned} \tag{2}$$

Here, n_{exc}, n_p, n_{cpf}, and n_{cpi} are exciton, polaron, and charge pair densities generated with the applied field and without it, respectively. $\Delta\alpha_{ex}$ and $\Delta\alpha_{cpi}$ are the differences of the exciton and impurity caused charge pair polarizabilities compared with those in the ground state, q is the electron charge, l_p is the charge separation distance, and $l(t)$ is the polaron drift distance. Since the charge pairs created by the exciton splitting on impurities are randomly oriented, the average charge separation distance along the electric field is zero (unclear). Therefore, we assume that they contribute to the field kinetics only by the displacement current due to the altered polarizabilty. On the contrary, charge pairs created by the field-assisted exciton splitting are oriented along the electric field. During the field-assisted charge pair generation, charge carriers drift along the electric field direction and contribute to the conduction current. Taking into account that free charge carriers can also be trapped after drifting some distance, we cannot clearly discriminate between free carrier and field-created bound charge pair contributions.

Exciton Contribution

Figure 1c shows the induced transient absorption kinetics determined at 810 nm. From the decay rate of the induced absorption observed at 810 nm, we can conclude that it is caused by excitons, since the relaxation kinetics of charge pairs is much slower [14]. The transient absorption kinetics in Figure 1c is identical within the experimental accuracy to the field kinetics at the 3-V applied voltage. Thus, the field kinetics at low applied voltages can be attributed to excitons. The field-induced charge pair and free polaron generation efficiencies are negligible at low applied voltages. This is in agreement with the threshold-like charge photogeneration efficiency dependence on the applied field determined in MeLPPP [15]. Charge pair generation on impurities is also evidently insignificant in the encapsulated sample, because, both in the transient absorption and the electric field kinetics, we do not observe any signal with a long lifetime which could be attributed to charge pairs. Thus, only excitons, polarons, and charge pair states created by the field-induced exciton splitting contribute significantly to the photocurrent in the encapsulated sample.

According to Eq. (2), the exciton contribution scales proportionally to the applied voltage. This allows us to determine the exciton contribution at higher fields. It equals to the transient absorption obtained at some particular applied voltage scaled by the same scaling factor, as used to normalize the transient absorption at 3 V (Fig. 1c) and multiplied by the applied voltage. By subtracting the exciton part from the total electric field kinetics, we obtain a free polaron and a field-separated charge pair part and decompose the field kinetics into the displacement and conductivity contributions as shown in Figure 2. The displacement contribution decays on a ps time scale simultaneously with the exciton concentration decay. Two phases with significantly different rates can be distinguished in the field dynamics related to polarons. As was shown in [15], the polaron generation by exciton quenching dominantly takes place on a tens-of-ps time scale with a decreasing rate. Therefore, the dynamics observed during the initial tens of ps should be assigned to the polaron generation, while the dynamics on a ns time scale should be assigned to the carrier drift increasing the charge separation distance. The initial separation distance, which is about 1 nm in the MeLPPP polymer [9], determines the field reduction value on a hundreds-of-ps time scale. The separation distance increases about 1.5–2 times during subsequent 3 ns due to the carrier drift in the electric field. It has been demonstrated that only a fraction of about 30% of the field-splitted excitons creates mobile charge carriers, which may be extracted from the sample, while

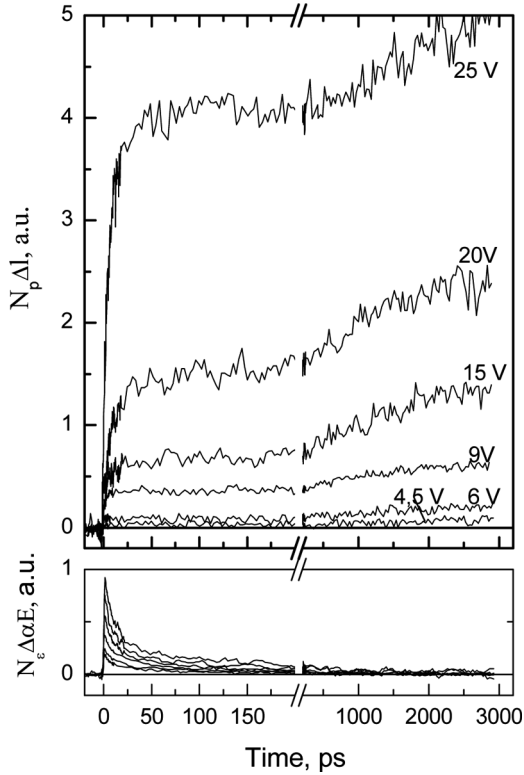

FIGURE 2 Conductivity (a) and displacement; (b) current contributions to the electric field dynamics in a capsulated MeLPPP sample. Voltages in (b) are the same as in (a) from the top down.

another fraction remains in coulombically bound charge pairs [16]. Thus, the charge pair contribution to the field kinetics during their generation time can be comparable or even larger than that of the free charge carrier current.

Impurity Role

Similar decomposition of the field kinetics in the nonprotected sample gives significantly different relative conductivity and displacement current contributions. The displacement contribution is similar to that observed in the protected sample (Fig. 2b), while the conductivity contribution is about three times lower (Fig. 2a). Moreover, the transient absorption in this sample has a slowly relaxing component (Fig. 3b). We attribute it to the states created by participation of impurities

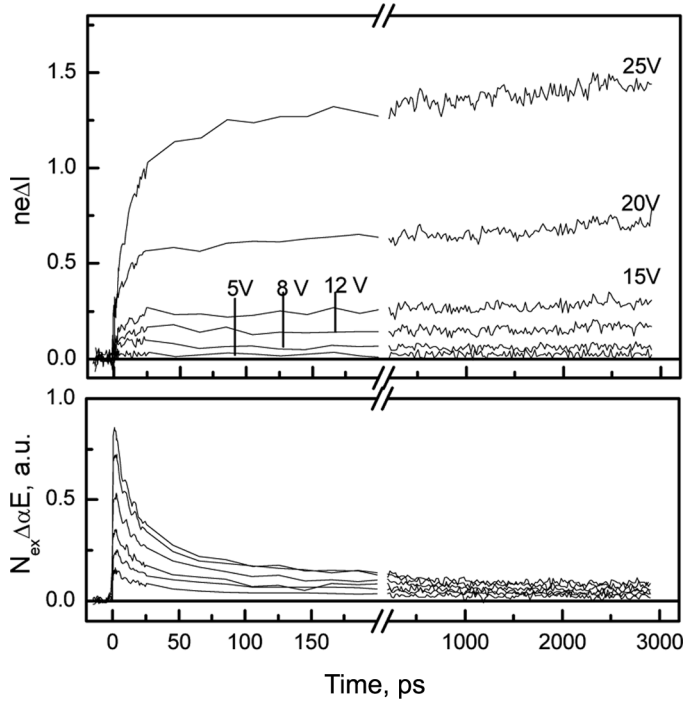

FIGURE 3 Conductivity (a) and displacement; (b) current contributions to the electric field dynamics in a noncapsulated MeLPPP sample. Voltages in (b) are the same as in (a) from the top down.

adsorbed from air, evidently oxidized polymer segments. Tightly bound charge pairs are evidently created at oxidized MeLPPP segments. Due to a much larger impurity density, the charge pair state density is also much higher in the nonprotected sample. As was demonstrated in [14], the formation of these states competes with the field-induced exciton splitting, reduces the free carrier generation yield, and, consequently, as we determine here, reduces the conductivity current.

It should be noted that the displacement current can be observed only in experiments with high time resolution. In experiments with the time resolution lower than the exciton life-time, the positive current during the exciton creation is compensated by the negative current appearing during the exciton relaxation. The relative contribution of the displacement current is particularly large at low applied voltages, when due to threshold-like charge carrier generation efficiency [15], the conductivity current is still weak. Since the displacement current is not related to the charge carrier generation,

its relative contribution should be higher in systems with a low carrier generation efficiency.

CONCLUSIONS

Conductivity and displacement currents are responsible for the photoconductivity in MeLPPP on a picosecond time scale. The displacement current contribution to the total current dynamics on a ps time scale is comparable to that of the conductivity current, or even dominating at low electric fields when the carrier photogeneration yield is low. The displacement contribution to the electric field appears simultaneously with the excitation pulse during the exciton generation and disappears simultaneously with the decay of excitons on a ps time scale, therefore the displacement contribution can be observed in measurements with high time resolution. The conductivity current appears with the polaron generation, and its kinetics is determined by the carrier concentration and the time-dependent mobility. In agreement with the earlier work [14], oxidation defects reduce the field-induced charge carrier generation and reduce the conductivity current.

REFERENCES

[1] Hertel, D. & Bässler, H. (2008). *Chem. Phys. Chem.*, *9*, 666.
[2] Borsenberger, P. M., Pautmeier, L., Richert, R., & Bässler, H. (1991). *J. Chem. Phys.*, *94*, 8276.
[3] Laquai, F. & Hertel, D. (2007). *Appl. Phys. Lett.*, *90*, 142109.
[4] Pasveer, W. F., Cottaar, J., Tanase, C., Coehoorn, R., Bobbert, P. A., Blom, P. W. M., de Leeuw, D. M., & Michels, M. A. J. (2005). *Phys. Rev. Lett.*, *94*, 206601.
[5] Hoofman, R. J. O. M., de Haas, M. P., Siebbeles, L. D. A., & Warman, J. M. (1998). *Nature*, *392*, 54.
[6] Hendry, E., Koeberg, M., Schins, J. M., Nienhuys, H. K., Sundström, V., Siebbeles, L. D. A., & Bonn, M. (2005). *Phys. Rev. B*, *71*, 125201.
[7] Gulbinas, V., Kananavicius, R., Valkunas, L., & Bassler, H. (2002). *Phys. Rev. B*, *66*, 233203.
[8] Gulbinas, V., Bassler, H., Yartsev, A., Zaushitsyn, Y., & Sundström. V. (2003). *Proc. SPIE*, *5122*, 156.
[9] Moses, D., Okumoto, H., Lee, C. H., & Heeger, A. J. (1996). *Phys. Rev. B*, *54*, 4748.
[10] Cabanillas-Gonzalez, J., Virgili, T., Gambetta, A., Lanzani, G., Anthopoulos, T. D., & de Leeuw, D. M. (2006). *Phys. Rev. Lett.*, *96*, 106601.
[11] Devižis, A., Serbenta, A., Meerholz, K., Hertel, D., & Gulbinas, V. *To be published*.
[12] Scherf, U. (1992). *Macromol. Chem.*, *193*, 1127.
[13] Gulbinas, V., Hertel, D., Yartsev, A., & Sundström, V. (2007). *Phys. Rev. B*, *76*, 235203.
[14] Gulbinas, V., Zaushitsyn, Y., Sundström, V., Hertel, D., Bässler, H., & Yartsev, A. (2002). *Phys. Rev. Lett.*, *89*, 107401–1.
[15] Hertel, D., Soh, E. V., Bässler, H., & Rothberg, L. J. (2002). *Chem. Phys. Lett.*, *361*, 99.